



University of Groningen

## Palladium alkyl complexes with a formazanate ligand

Milocco, Francesca; de Vries, Folkert; Dall'Anese, Anna; Rosar, Vera; Zangrando, Ennio; Otten, Edwin; Milani, Barbara

*Published in:*  
Dalton Transactions

*DOI:*  
[10.1039/c8dt03130d](https://doi.org/10.1039/c8dt03130d)

**IMPORTANT NOTE:** You are advised to consult the publisher's version (publisher's PDF) if you wish to cite from it. Please check the document version below.

*Document Version*  
Final author's version (accepted by publisher, after peer review)

*Publication date:*  
2018

[Link to publication in University of Groningen/UMCG research database](#)

### *Citation for published version (APA):*

Milocco, F., de Vries, F., Dall'Anese, A., Rosar, V., Zangrando, E., Otten, E., & Milani, B. (2018). Palladium alkyl complexes with a formazanate ligand: Synthesis, structure and reactivity. *Dalton Transactions*, 47(41), 14445-14451. <https://doi.org/10.1039/c8dt03130d>

### **Copyright**

Other than for strictly personal use, it is not permitted to download or to forward/distribute the text or part of it without the consent of the author(s) and/or copyright holder(s), unless the work is under an open content license (like Creative Commons).

### **Take-down policy**

If you believe that this document breaches copyright please contact us providing details, and we will remove access to the work immediately and investigate your claim.

*Downloaded from the University of Groningen/UMCG research database (Pure): <http://www.rug.nl/research/portal>. For technical reasons the number of authors shown on this cover page is limited to 10 maximum.*

# Palladium Complexes with Formazanate Ligands: Synthesis, Structures and Reactivity

*Francesca Milocco,<sup>†,‡</sup> Folkert de Vries,<sup>†,‡</sup> Anna Dall'Anese,<sup>‡</sup> Vera Rosar,<sup>‡\*</sup> Ennio Zangrando,<sup>‡</sup>  
Edwin Otten<sup>\*,†</sup> and Barbara Milani<sup>\*,‡</sup>*

<sup>‡</sup> Dipartimento di Scienze Chimiche e Farmaceutiche, Università di Trieste, Via Licio Giorgieri  
1, 34127 Trieste, Italy

<sup>†</sup> Stratingh Institute for Chemistry, University of Groningen, Nijenborgh 4, 9747 AG Groningen,  
The Netherlands

<sup>\*</sup>Current address: Department of Chemistry and Biochemistry, University of Bern, Freiestrasse 3,  
3012 Bern, Switzerland

Palladium(II) complexes with a bidentate, anionic formazanate ligand are described. The homoleptic bis(formazanate) palladium complex is easily obtained, also when attempting to prepare mono(formazanate) complexes by protonolysis or salt metathesis reactions. It shows rich electrochemistry due to the redox-active nature of the ligands. Performing salt metathesis between the precursor  $[\text{Pd}(\text{COD})(\text{CH}_3)\text{Cl}]$  and the potassium salt of the ligand in the presence of tetrabutylammonium chloride allows the high-yield synthesis of a square planar mono(formazanate) palladate complex through coordination of chloride anion. Dissociation of  $\text{Cl}^-$  allows binding of unsaturated molecules and evaluation of the reactivity of the (formazanate) $\text{Pd}(\text{CH}_3)$  fragment. Using this approach, insertion reactions of CO, isocyanide and methyl acrylate into the  $\text{Pd}-\text{CH}_3$  bond are demonstrated.

## Introduction

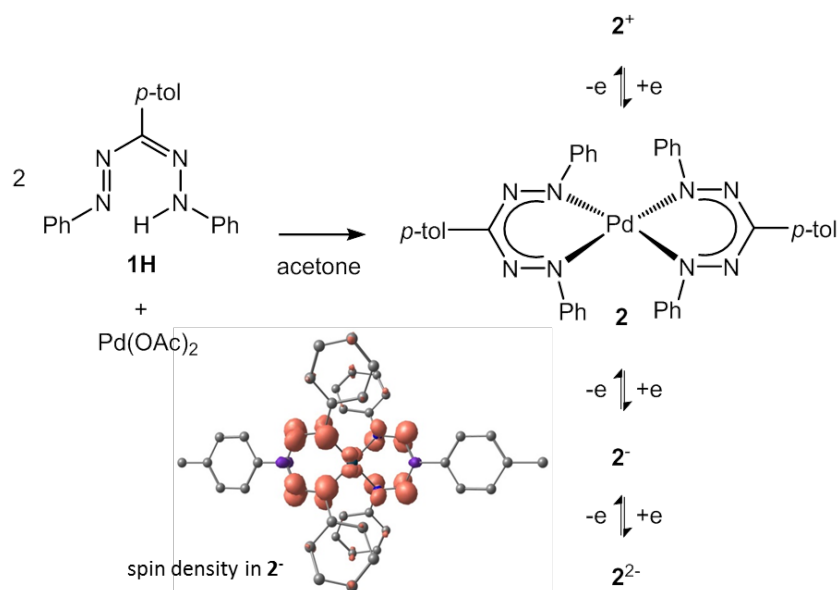
Alkylpalladium complexes with either neutral or mono-anionic bidentate ligands are well-known for their ability to catalyze olefin oligomerization/polymerization. In particular, these catalysts show a remarkable tolerance to polar functional groups in comparison to early transition metal catalysts. Therefore, they have been studied extensively for coordination-insertion type copolymerization of ethylene with polar vinyl monomers, leading to polyolefins that incorporate functional groups in the polymer chain.<sup>1</sup> Following the pioneering work by Brookhart and co-workers on catalysts containing sterically demanding neutral  $\alpha$ -diimine ligands,<sup>2</sup> much research has been performed on these systems to arrive at a thorough understanding of mechanistic details and structure/activity relationships.<sup>3</sup> Our long-standing interest in this type of catalysis has focused on the design of neutral N-donor ligands to improve catalyst activity/stability and obtain products with improved properties.<sup>4</sup> Nickel(II) and palladium(II) compounds with mono-anionic bidentate ligands are also known as active catalysts for olefin polymerization (e.g., with phosphino-sulfonate<sup>5</sup> or salicylaldimine ligands),<sup>6</sup> but, surprisingly, complexes with monoanionic nitrogen-based ligands such as  $\beta$ -diiminates have been comparatively little studied in group 10 chemistry.<sup>7</sup> This is equally true for the nitrogen-rich analogues of  $\beta$ -diiminates, such as 1,2,4,5-tetrazapentadienyl ligands (with NNCNN backbone) that are better known as ‘formazanates’.<sup>8</sup> Although the latter ligands have been sporadically used in coordination compounds with Ni(II)<sup>9</sup> and Pd(II),<sup>10</sup> it is only recently that they have gained renewed interest due to their unusual redox- and optoelectronic properties.<sup>11,12,13</sup> Aiming to exploit the tunable steric and electronic properties of formazanate ligands in palladium catalysis, we report here the synthesis and characterization of formazanate palladium complexes. This includes the first example of a methylpalladium complex with a

formazanate ligand, and a study of insertion of unsaturated substrates (CO, isocyanide and methyl acrylate) in the Pd-C bond in this system.

## Results and Discussion

**Synthesis and characterization of a bis(formazanate)palladium complex.** Treatment of palladium(II) acetate with 2 equiv of formazan **1H** in acetone resulted in a dark red solution which was stirred at room temperature for 5 h. Upon concentration of the reaction mixture and storage in the fridge overnight, a dark solid precipitated which was isolated by filtration. The  $^1\text{H}$  NMR spectrum recorded in  $\text{CD}_2\text{Cl}_2$  at 25 °C only showed the signals for the formazanate ligand, with the exception of the NH. The number of signals and their integration were typical of a symmetrical bischelated structure, indicating that the isolated solid corresponded to the bis(formazanate)palladium complex **2**,  $[\text{Pd}(\mathbf{1})_2]$  (Scheme 1).

**Scheme 1.** Synthesis of compound **2**, showing the electrochemically observed redox-series  $\mathbf{2}^{+/0/-1/2}$  and representation of the spin density distribution (isosurface 0.004 a.u.) in  $\mathbf{2}^-$ .



The infrared spectrum of **2** contained bands at  $1198\text{ cm}^{-1}$  and  $1269\text{ cm}^{-1}$  due to N-N and C-N stretching in the ligand backbone, respectively. These values were in agreement with those reported by Siedle for the related bis(formazanate)palladium complexes ( $v_{\text{max}}$  (stretching N-N) =  $1200\text{ cm}^{-1}$ ,  $v_{\text{max}}$  (stretching C-N) =  $1275\text{ cm}^{-1}$ ).<sup>10a</sup> Slow diffusion of *n*-hexane into a chloroform solution of **2** at  $4\text{ }^{\circ}\text{C}$  afforded single crystals suitable for X-ray crystallography. The structural analysis confirmed that **2** contains a palladium ion coordinated by the terminal nitrogen atoms of two formazanate ligands in a square planar coordination environment (Figure 1, pertinent bond lengths and angles in Table 1). The two formazanate ligands are related by symmetry, as the palladium atom is located on an inversion center.

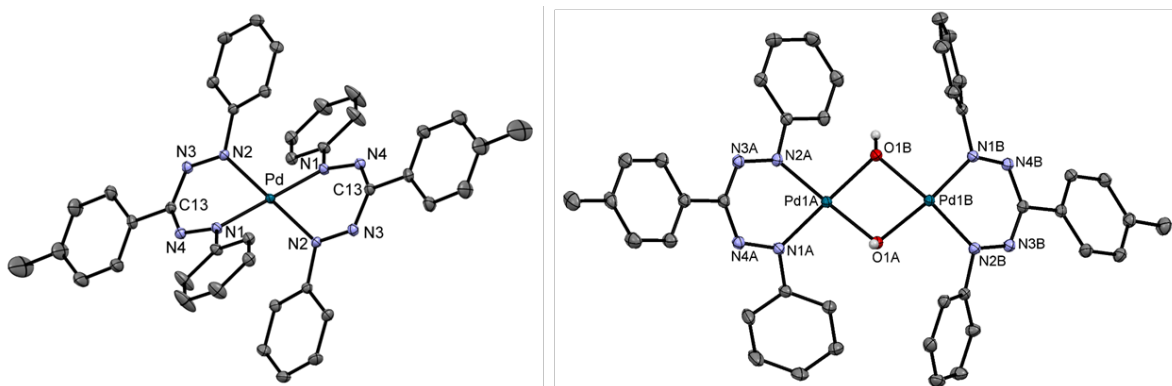


**Figure 1.** ORTEP drawing (ellipsoids at 50% probability) of compounds **2** (left) and **3** (right) with atom labeling scheme of the non-C atoms. Hydrogen atoms (except for the OH groups in **3**) are omitted for clarity.

**Table 1.** Selected bond lengths (Å) and angles (°) in compounds **2**, **3** and **5**.

	<b>2</b>	<b>3</b>		<b>5</b>
	(x = none)	(x = A)	(x = B)	(x = none)
Pd(1x)-N(1x)	2.0265(13)	1.992(2)	1.963(2)	2.033(3)
Pd(1x)-N(2x)	2.0162(13)	1.991(2)	1.975(2)	2.117(3)
Pd(1x)-O(1A)		2.0317(18)	2.0428(18)	
Pd(1x)-O(1B)		2.0567(18)	2.0781(18)	
Pd(1)-Cl(1)				2.3055(10)
Pd(1)-C(21)				2.062(3)
N(1x)-N(4x)	1.2956(16)	1.291(3)	1.285(3)	1.293(4)
N(2x)-N(3x)	1.2925(15)	1.291(3)	1.289(3)	1.297(4)
N(3x)-C(13x)	1.3507(18)	1.343(3)	1.345(3)	1.363(4)
N(4x)-C(13x)	1.3426(18)	1.356(3)	1.350(3)	1.352(5)
N(1x)-Pd(1x)-N(2x)	82.04(6)	82.92(9)	88.87(9)	82.37(12)
$\angle(\text{N-Pd-N})/(\text{X-Pd-X})^a$	0.00	5.09	7.83	5.28

<sup>a</sup> Dihedral angle between the coordination planes defined by the N-Pd-N and X-Pd-X atoms.

The two formazanate ligands are coordinated to the metal center in such a way that no  $\pi$ -stacking interaction is observed among the aromatic rings of the two ligands. Full delocalization within the formazanates is indicated by the equivalent N-N and C-N bond lengths in the backbone of each ligand (Table 1). The Pd-N bond lengths are 2.0265(13) and 2.0162(13) Å and the PdN<sub>2</sub> coordination plane forms a dihedral angle of 42.08° with the mean plane through the N<sub>4</sub>C backbone of the ligand (Figure S1). These structural features closely resemble those found in the bis(3-nitroformazanate)nickel<sup>9b</sup> and bis(1,3,5-triarylformazanate)palladium complexes<sup>10a</sup> prepared previously.

Given the redox non-innocence of formazanate ligands in coordination complexes, we investigated the electrochemical properties of complex **2** by cyclic voltammetry. The cyclic voltammogram shows two quasi-reversible reductions taking place at -1.47 and -1.82 V vs  $\text{Fc}^{0/+}$  ( $\text{Fc}$  = ferrocene), that correspond to the transformation of **2** to the radical anion  $\mathbf{2}^{\cdot-}$  and subsequently to the dianion  $\mathbf{2}^{2-}$ , respectively (Figure 2).

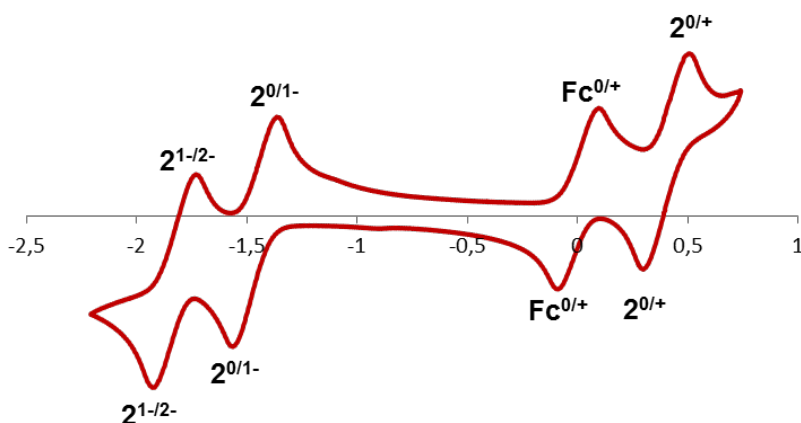


**Figure 2.** Cyclic voltammogram of compound **2** (ca. 1.50 mM solution of **2** in THF; 0.1 M  $[\text{nBu}_4\text{N}][\text{PF}_6]$  electrolyte; scan rate =  $0.5 \text{ V}\cdot\text{s}^{-1}$ ).

The observed reductions are shifted to more negative potentials compared to the corresponding bis(formazanate)zinc complexes ( $-1.39$  and  $-1.68 \text{ V vs Fc}^{0/+}$ ),<sup>11a</sup> which is likely due to a difference in electronegativity of Pd(II) vs. Zn(II). In addition to the two sequential reduction events, the cyclic voltammogram of **2** shows a quasi-reversible oxidation at  $+0.41 \text{ V vs Fc}^{0/+}$ , related to the redox couple  $\mathbf{2}^{0/1+}$ , which is absent in the zinc analogues.<sup>11a,14</sup> The cyclic voltammetry of **2** is similar in overall appearance to that observed for Pd(II) complexes with redox-active ortho-aminophenolate ligands,<sup>15</sup> albeit that the redox-potentials in **2** are all shifted towards more negative potentials. Geometry optimizations for  $\mathbf{2}^{\cdot-}$  at the DFT (B3LYP/6-

31+G(d,p) (C,H,N) LANL2DZ (Pd)) level of theory converge at a square planar geometry with a slight elongation of Pd-N bonds (calculated: 2.109 Å for **2**<sup>-</sup> vs. 2.078 Å for **2**) and somewhat longer N-N bonds in the ligand (1.311 Å for **2**<sup>-</sup> vs. 1.288 Å for **2**). A spin density plot of the radical **2**<sup>-</sup> shows that the majority is found on the formazanate N-atoms, but, in contrast to the tetrahedral Zn analogues, there is also a noticeable spin density on the Pd center (Scheme 1). Similarly, in the case of the cation **2**<sup>+</sup> most spin density resides in the ligand with a small contribution on the Pd center, indicating that also the oxidation event is a ligand-based reaction (Figure S3). Scanning further towards more negative potentials reveals additional reduction events, but these appeared to be much less reversible (Figure S47). From this it is clear that **2** is stable in a range of different oxidation states (**2**<sup>1+/0/1-/2-</sup>, Scheme 1), which is the result of ligand-based redox reactions. The electrochemical behavior of **2** differs from that reported by Hicks et al. for (3-nitroformazanate)palladium hexafluoroacetylacetonate complexes,<sup>10b</sup> for which irreversible reductions were observed. Conversely, our data suggest that relatively stable 1- and 2-electron reduction products of bis(formazanate) complexes with divalent metal ions may be a general feature of this ligand class.

It is known from the literature that bischelated palladium(II) complexes with neutral nitrogen-donor chelating ligands [Pd(N-N)<sub>2</sub>][PF<sub>6</sub>]<sub>2</sub>, such as 1,10-phenanthroline and 2,2'-bipyridine, generate highly active catalysts for the CO/vinyl arene copolymerization reaction yielding perfectly alternating polyketones.<sup>16</sup> Therefore, complex **2** was tested in the CO/styrene and CO/4-methylstyrene copolymerization. The catalytic reaction was performed in 2,2,2,-trifluoroethanol with the addition of 1,4-benzoquinone (BQ) ([BQ]/[Pd] = 5) as an oxidant, at different temperatures and pressures (Table S1). In all cases after 24 h of reaction no polyketone was formed, and there was no indication of the formation of inactive palladium metal. <sup>1</sup>H NMR



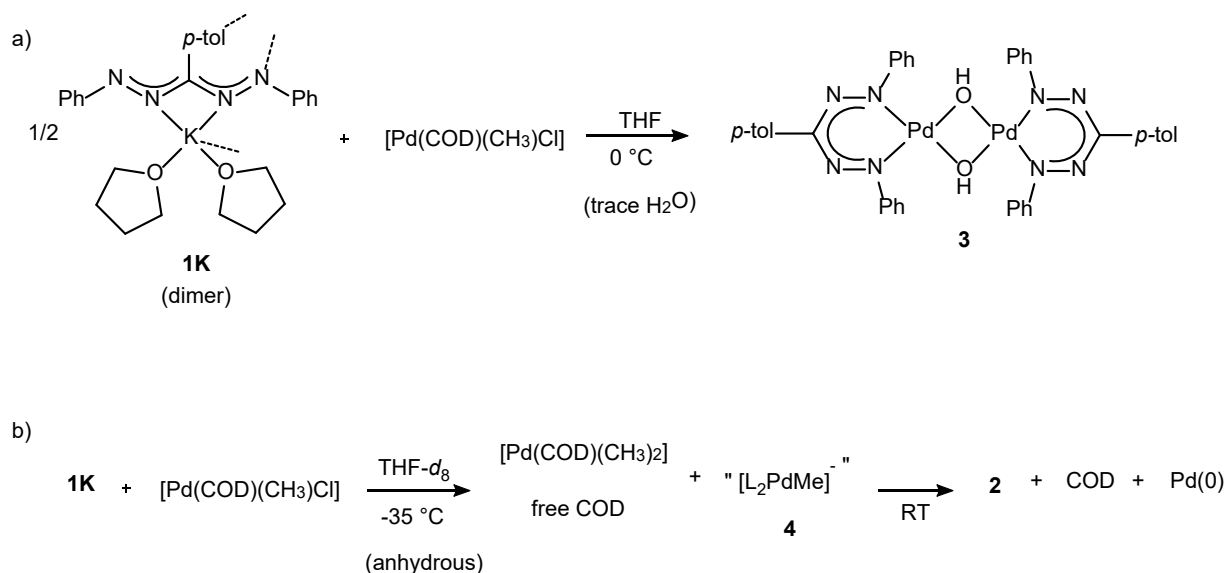
analysis of the solid obtained from the work up of the catalytic mixture evidenced that the precatalyst, compound **2**, was recovered. The lack of reactivity of **2** prompted us to attempt the synthesis of mono(formazanate)palladium complexes, where access to species with a vacant coordination site in the palladium coordination sphere could lead to coordination-insertion type reactions, such as shown for neutral Pd(II) complexes with anionic chelating phosphino-sulfonate ligands.<sup>5</sup>

**Synthesis and characterization of mono(formazanate)palladium complexes.** Palladium complexes with one bidentate anionic nitrogen-donor ligand have been reported in the literature, for example with the  $\beta$ -diiminate ligand. Bercaw and co-workers observed insertion of COD (1,5-*cis,cis*-cyclooctadiene) into the Pd-C bond of the transient species ( $\beta$ -diiminate)Pd(CH<sub>3</sub>)(COD).<sup>17</sup> A competing C-H activation with the solvent (benzene) was also observed to give the product of insertion into a Pd-Ph bond, while performing the reaction in the presence of acetonitrile afforded the adduct ( $\beta$ -diiminate)Pd(CH<sub>3</sub>)(CH<sub>3</sub>CN). Pörschke and co-workers described attempts to synthesize  $\beta$ -diiminate palladium chloride complexes (with N-isopropyl substituents), which led to formation of palladium black and oxidative coupling of the  $\beta$ -diiminate ligand.<sup>18</sup> Subsequently, the Song group has successfully prepared a variety of N-aryl substituted mono( $\beta$ -diiminate)palladium complexes and studied their reactivity.<sup>19</sup>

The reaction of the potassium formazanate salt **1K**<sup>20</sup> with [Pd(COD)(CH<sub>3</sub>)Cl] was initially evaluated (Scheme 2). Compound **1K** (0.5 eq of the dimeric potassium salt, 1 eq of formazanate anion) was added to a THF (commercial ‘anhydrous’ grade) solution of [Pd(COD)(CH<sub>3</sub>)Cl] (1 eq) and the reaction mixture was stirred at room temperature for 30 min. After concentration and precipitation with *n*-hexane, a blue solid was obtained. The <sup>1</sup>H NMR spectrum of the crude

product shows the presence of two species: signals for **2** (the major product) and a new species (**3**) that shows two singlets at -3.46 and 2.36 ppm in the upfield part of the spectrum (Figure S7).

**Scheme 2.** Reactions of **1K** with  $[\text{Pd}(\text{COD})(\text{CH}_3)\text{Cl}]$ .\*



\* a) in the presence of traces of water; b) in anhydrous THF

Repeating the reaction at 0 °C, precipitation with hexane and workup of the soluble fraction allowed isolation of a solid product in which **3** was present as the major species (Figure S8). Crystals of **3** were eventually obtained by slow diffusion of hexane into an NMR sample in  $\text{CD}_2\text{Cl}_2$ . X-ray diffraction studies showed compound **3** to be the dimeric complex  $[(\mathbf{1})\text{Pd}(\mu\text{-OH})_2]$ , in which the palladium centers are connected by two bridging hydroxo groups (Figure 1). Both halves of the dimer show somewhat different metrical parameters (e.g., Pd(2) shows slightly longer Pd-N distances but shorter Pd-O distances in comparison to Pd(1), see Table 1). The Pd ions exhibit a square planar coordination geometry with Pd-N and Pd-O bond distances ranging from 1.963(2) to 1.991(2) Å, and from 2.0323(18) to 2.0784(18) Å, respectively (Table 1). The distance between both Pd atoms is 3.0490(8) Å. A similar  $\mu$ -hydroxide complex was

reported with nickel(II) and sterically demanding 3-nitro- or 3-cyanoformazanate ligands,<sup>9b</sup> and a related palladium(II) complex with a  $\beta$ -diiminate ligand is known.<sup>19b</sup> The origin of the hydroxide groups in **3** is likely a trace amount of water present in the reaction solvent, or introduced during workup. These hydroxides account for the upfield <sup>1</sup>H NMR signal at  $\delta$  -3.46 ppm, which was further supported by its disappearance upon addition of D<sub>2</sub>O (other peaks remained unchanged), indicating that there is exchange between the  $\mu$ -OH fragment and D<sub>2</sub>O.

Subsequently, we probed the reaction **1K** with [Pd(COD)(CH<sub>3</sub>)Cl] under strictly anhydrous conditions by performing NMR scale reactions in a glovebox using THF-*d*<sub>8</sub> as the solvent (distilled from Na/K alloy). Addition of a cold (-35 °C) solution of **1K** in THF-*d*<sub>8</sub> to [Pd(COD)(CH<sub>3</sub>)Cl] (formazanate: Pd ratio of 1:1) resulted in immediate color change from dark red to blue. The sample was quickly frozen in liquid nitrogen and subsequently inserted into an NMR probe pre-cooled to -40 °C. In the initial <sup>1</sup>H NMR spectrum no signal of the starting materials is present, and only a trace amount of the bis(formazanate)palladium complex **2** is observed. Although a complex mixture is obtained, free cyclooctadiene and the palladium compound [Pd(COD)(CH<sub>3</sub>)<sub>2</sub>] (in THF-*d*<sub>8</sub>, Pd-CH<sub>3</sub> <sup>1</sup>H NMR: 0.22 ppm; <sup>13</sup>C NMR: 3.15 ppm)<sup>21,22</sup> are unambiguously identified in the spectra (Figure 3). Judging by the multitude of signals observed in the aromatic region, several new formazanate-containing species are present. A new <sup>1</sup>H NMR singlet resonance at -0.05 ppm (<sup>13</sup>C: -5.7 ppm) suggests that at least one new product with a Pd-CH<sub>3</sub> moiety is formed (compound **4**): its chemical shift is in the range for a methylpalladate complex (*vide infra*, **5**). The lack of dipolar coupling (NOESY NMR) between this Pd-CH<sub>3</sub> group and the region in which COD resonances are expected suggests that **4** does not contain a COD ligand. Moreover, the absence of new signals between 4 and 5.5 ppm argues against a cyclooctenyl-species derived from COD insertion, a product which was observed in

related  $\beta$ -diiminate chemistry.<sup>17</sup> On the basis of this, we tentatively assign species **4** as the anionic complex  $[(\mathbf{1})_2\text{Pd}(\text{CH}_3)]^-$ , in which one of the formazanate fragments is likely to be monodentate.

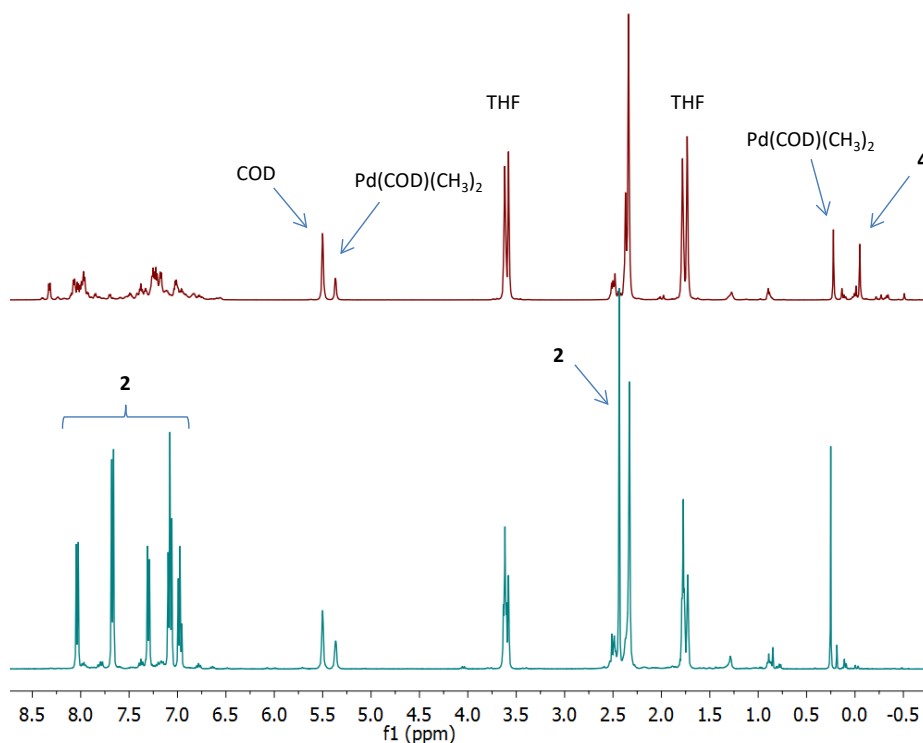
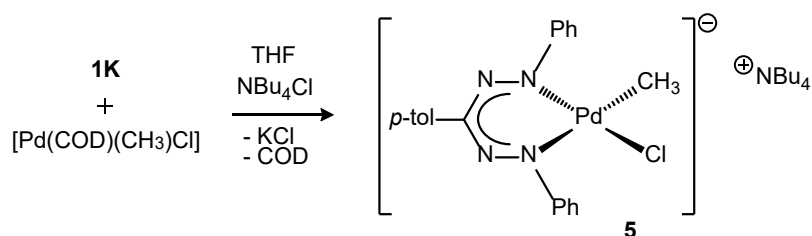


**Figure 3.**  $^1\text{H}$  NMR spectra of **1K** +  $[\text{Pd}(\text{COD})(\text{CH}_3)\text{Cl}]$  in distilled  $\text{THF-}d_8$ , immediately after mixing at  $-40\text{ }^\circ\text{C}$  (top) and after standing at room temperature for 1 day (bottom).

Upon warming the NMR sample to room temperature, full conversion to the bis(formazanate)palladium complex **2** is observed in 24 h. In the  $^1\text{H}$  NMR spectrum, resonances attributable to **2**,  $[\text{Pd}(\text{COD})(\text{CH}_3)_2]$  and free COD together account for  $> 90\%$  of the total signal intensity.

Attempted protonolysis of  $[\text{Pd}(\text{COD})(\text{CH}_3)\text{Cl}]$  with the free formazan **1H** in an NMR tube in  $\text{CD}_2\text{Cl}_2$  solution gave no reaction. Addition of excess triethyl amine to the **1H**/ $[\text{Pd}(\text{COD})(\text{CH}_3)\text{Cl}]$  mixture in  $\text{CD}_2\text{Cl}_2$  resulted in gradual disappearance of the starting material and formation of **2**, together with minor (as yet unidentified) palladium species. Taken together, the experiments described above indicate that simple salt metathesis or protonolysis protocols do not lead to clean formation of mono(formazanate)palladium complexes, likely because the bis(formazanate) complex **2** is a thermodynamic sink in these reactions.

**Scheme 3.** Synthesis of **5** via salt metathesis in the presence of tetrabutylammonium chloride.



Based on these results, we hypothesized that successful synthesis of a mono(formazanate)palladium complex would require stabilization of the coordinatively unsaturated intermediate  $[(\mathbf{1})\text{Pd}(\text{CH}_3)]$  to prevent its conversion to **2**. Thus, we examined the reaction of **1K** with  $[\text{Pd}(\text{COD})(\text{CH}_3)\text{Cl}]$  in the presence of one equivalent of tetrabutylammonium chloride. After stirring for 2 hours, filtration and diffusion of hexane into the THF solution afforded dark blue crystals of the product  $[\text{Bu}_4\text{N}][(\mathbf{1})\text{Pd}(\text{CH}_3)\text{Cl}]$  (**5**) in 83% isolated yield.  $^1\text{H}$  NMR spectroscopy showed a characteristic Pd- $\text{CH}_3$  resonance at -0.02 ppm ( $^{13}\text{C}$  NMR: -5.0 ppm), and the observed integration was consistent with a formazanate: Pd- $\text{CH}_3$  ratio of 1:1. The NMR spectra of **5** indicate that the two halves of the formazanate ligand are inequivalent, as expected for a square planar complex with Pd- $\text{CH}_3$  and Pd-Cl ligands.

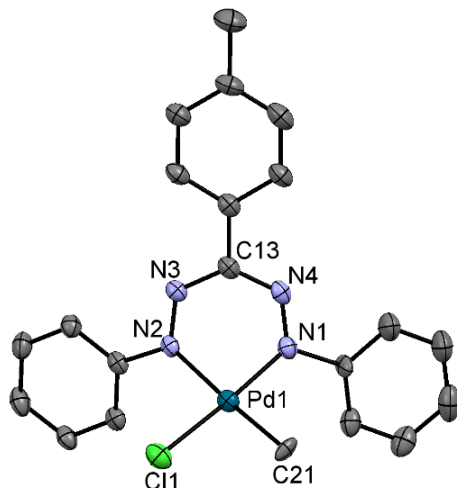


**Figure 4.** ORTEP drawing (ellipsoids at 50% probability) of compound **5**. Hydrogen atoms and the  $\text{Bu}_4\text{N}^+$  cation are omitted for clarity.

An X-ray diffraction study confirmed the proposed formulation (Figure 4, pertinent bond lengths and angles in Table 1). The anionic part of the molecule consists of a square planar Pd center bound to a bidentate formazanate, a chloride and methyl ligand. The metrical parameters in the formazanate ligand in **5** are unsurprising, and closely resemble those in **2** and **3**. Cyclic voltammetry in THF solution (0.1 M  $[\text{Bu}_4\text{N}][\text{PF}_6]$  as electrolyte) shows that **5** possesses a quasi-reversible reduction wave at  $E_{1/2} = -1.87$  V vs.  $\text{Fc}^{0/+}$  (Figure S48), which is likely a ligand-based event; the 400 mV shift to more negative potential than observed for **2** is consistent with the overall charge of -1 for palladate complex **5**. Somewhat surprisingly, the quasi-reversible nature indicates that the electrochemically generated radical dianion  $[(\mathbf{1})\text{Pd}(\text{CH}_3)\text{Cl}]^{2-}$  does not lose  $\text{Cl}^-$  on the timescale of the voltammetry experiment.

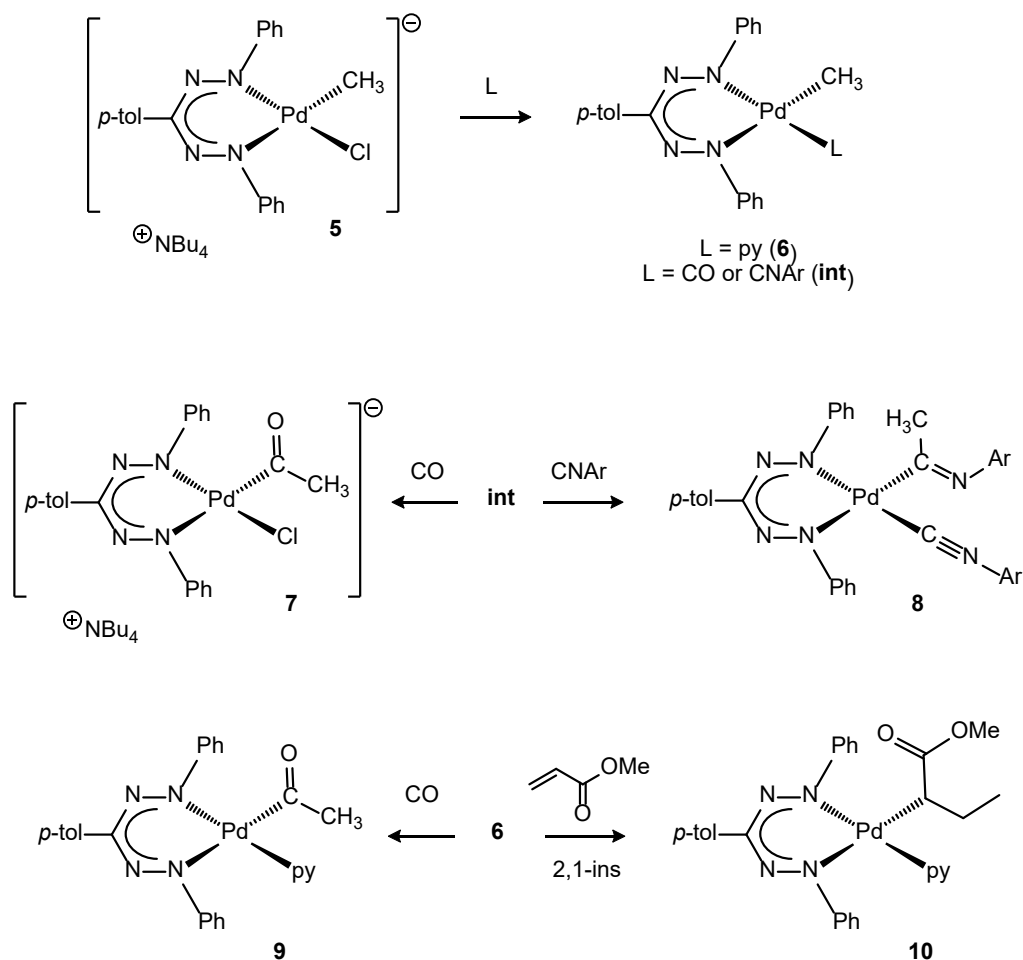
The straightforward synthesis of **5** confirms that transmetalation between **1K** and  $[\text{Pd}(\text{COD})(\text{CH}_3)\text{Cl}]$  is facile and indeed produces the target mono(formazanate)palladium compound. The neutral complex  $[(\mathbf{1})\text{Pd}(\text{CH}_3)]$  that is formed as an intermediate is apparently

unstable in the absence of a fourth ligand to complement the Pd coordination sphere. This is in agreement with data reported for  $\beta$ -diketiminato nickel compounds, which are stabilized by binding lutidine as neutral co-ligand or via  $\beta$ -agostic interactions with the alkyl group.<sup>23</sup> In our case, the presence of chloride ions leads to formation of a stable four-coordinate palladate complex. Such palladate species are also of current interest due to their involvement in cross-coupling catalysis.<sup>24</sup>

With the successful synthesis of **5** in hand, we wondered whether chloride abstraction would allow (transient) access to the putative three-coordinate compound  $[(\mathbf{1})\text{Pd}(\text{CH}_3)]$  and provide insight in the pathway of its conversion to **2** (*vide supra*). Thus, THF-*d*<sub>8</sub> solutions of **5** were reacted at -30 °C in three separate experiments with NaBPh<sub>4</sub>, AgBF<sub>4</sub> or B(C<sub>6</sub>F<sub>5</sub>)<sub>3</sub>, and the reactions were monitored by NMR spectroscopy at -40 °C. A detailed discussion of these experiments is provided in the Supporting Information. Here, we note that in none of these reactions we were able to unambiguously identify  $[(\mathbf{1})\text{Pd}(\text{CH}_3)]$  as a transient intermediate. The reaction with NaBPh<sub>4</sub> results in formation of **2** as the major product, presumably as a result of chloride abstraction from **5**. Similarly, B(C<sub>6</sub>F<sub>5</sub>)<sub>3</sub> reacts with **5** to form a 2:1 mixture of the borates  $[\text{ClB}(\text{C}_6\text{F}_5)_3]^-$  and  $[(\text{CH}_3)\text{B}(\text{C}_6\text{F}_5)_3]^-$  due to chloride/methyl abstraction from **5**; again, **2** is the major product in solution. Finally, the reaction with AgBF<sub>4</sub> does not lead to chloride abstraction, but the data indicate that electron-transfer could occur as evidenced by the formation of ethane and a species that we tentatively assign as the chloride-bridged dimer  $[(\mathbf{1})\text{Pd}(\mu\text{-Cl})_2]$ , for which there is precedent in related  $\beta$ -diiminato chemistry.<sup>25</sup>

**Ligand exchange and insertion reactions.** We subsequently evaluated ligand exchange and insertion reactions with the palladate complex **5** (Scheme 4). Stirring complex **5** with 2.6 equiv of pyridine in dichloromethane solution gave the neutral pyridine adduct [(1)Pd(CH<sub>3</sub>)(py)] (**6**), which was isolated in 46% yield. The <sup>1</sup>H NMR spectrum of **6** shows the singlet of the Pd-CH<sub>3</sub> group at 0.05 ppm, and inequivalent formazanate NPh groups, in agreement with the non-symmetrical chemical environment around palladium.

**Scheme 4.** Ligand exchange reactions with **5** and insertion of unsaturated substrates in the Pd-CH<sub>3</sub> bond.





Addition of excess CO to a THF-*d*<sub>8</sub> solution of compound **5** resulted in clean formation of the CO insertion product [Bu<sub>4</sub>N][(1)Pd(COCH<sub>3</sub>)Cl] (**7**), which shows NMR resonances at δ 2.33 (<sup>1</sup>H) and 235.5/37.4 ppm (<sup>13</sup>C) that are characteristic for the palladium acyl group.<sup>26</sup> A labelling experiment using <sup>13</sup>CO confirmed that the Pd-C resonance at 235.7 ppm in the <sup>13</sup>C NMR was enhanced due to the incorporation the <sup>13</sup>C label. Aside from free <sup>13</sup>CO, no other signals attributable to <sup>13</sup>C incorporation were observed, indicating that the chloride ligand is retained in the anionic product **7** rather than Cl/<sup>13</sup>CO exchange to give a neutral <sup>13</sup>C-labeled palladium carbonyl species. Treatment of **5** with 1 equiv of 4-methoxyphenyl isocyanide on NMR scale in THF-*d*<sub>8</sub> resulted in a mixture of products and some unreacted **5**, but addition of a second equivalent of isocyanide led to the formation of a single species according to NMR spectroscopy which was characterized as the isocyanide insertion product [(1)Pd(C(CH<sub>3</sub>)=NC<sub>6</sub>H<sub>4</sub>OCH<sub>3</sub>)(CNC<sub>6</sub>H<sub>4</sub>OCH<sub>3</sub>)] (**8**, Scheme 4). Diagnostic NMR data for **8** include a singlet at 2.41 ppm for the iminoacyl-CH<sub>3</sub> group, and a <sup>13</sup>C NMR signal at 184.5 ppm for the Pd-bound C=N carbon. Compounds **7** and **8** are both sufficiently stable to allow characterization by NMR spectroscopy, but solutions left at room temperature decompose in the course of several hours to unidentified species (including palladium black). Also the pyridine adduct **6** inserts CO, albeit more slowly than the anionic chloride **5**, to give compound **9** which shows acyl-CH<sub>3</sub> NMR resonances at δ 1.80 (<sup>1</sup>H) and 36.7 ppm (<sup>13</sup>C). The reaction of **6** with CO in the presence of additional pyridine (ca. 2.2 equiv) is qualitatively found to be slower than without added pyridine: in the former only 13% conversion of **6** is seen after 3 hours, while in the latter it reaches > 85% conversion in the same time. Based on these data, we propose that the reaction occurs by a dissociative pathway *via* a three-coordinate intermediate obtained by loss of the pyridine (in **6**) or chloride ligand (in **5**) to give the (unobservable) four-coordinate

intermediates (**int**) shown in Scheme 4. The subsequent insertion reactions are fast, and are followed by capture of the ‘best’ ligand in the mixture (i.e.,  $\text{CNC}_6\text{H}_4\text{OCH}_3 > \text{Cl}^- > \text{CO}$ ).

Finally, insertion of olefinic substrates was tested. Although addition of 1 bar of ethylene to compound **6** does not lead to observable changes in the NMR spectrum when followed over several days, the reaction of **6** with methyl acrylate slowly converts to a new species which is formulated as the 2,1-insertion product  $[(\mathbf{1})\text{Pd}(\text{CH}(\text{Et})\text{CO}_2\text{CH}_3)(\text{py})]$  (**10**) on the basis of its NMR spectral features. Specifically, the observation of a set of diastereotopic  $\text{CH}_2$  resonances in the  $^1\text{H}$  NMR spectrum at  $\delta$  1.25 and 1.06 ppm, which show scalar coupling to a Pd-bound CH (dd at  $\delta$  2.34 ppm) and a  $\text{CH}_3$  group (t at  $\delta$  0.70 ppm), is consistent with the proposed 2,1-insertion. Although cationic palladium complexes initially insert methyl acrylate with the same regiochemistry, subsequent  $\beta$ -hydride elimination and re-insertion events lead to six-membered chelate rings in which the  $\text{C}=\text{O}$  moiety is bound to Pd.<sup>1a,27</sup> For neutral phosphinosulfonate-ligated palladium compounds, 2,1-insertion of methyl acrylate is also favored, but in that case a subsequent 2,1-insertion occurs which allows formation of a stable six-membered chelate ring.<sup>28</sup> The observed insertion of methyl acrylate contrasts the finding of Novak and co-workers, who demonstrated that neutral palladium complexes with anionic pyrrole-imine ligands react with methyl acrylate via a radical mechanism instead of coordination-insertion.<sup>29</sup> Preliminary tests of stoichiometric and catalytic reactions with ethylene and CO/styrene with compounds **5** and **6** failed to provide evidence for sequential insertion reactions and formation of oligomeric/polymeric products. Spectroscopic analysis of the solid residue obtained after attempted CO/styrene copolymerization with **5** showed decomposition to **2** and free ligand. Although insertion of CO, isocyanides and olefins is well-documented with palladium(II) organometallics,<sup>4a,30</sup> the vast majority of these compounds contain neutral ligands (e.g.,

phosphines, bipyridines,  $\alpha$ -diimines), and organometallic palladium chemistry with anionic nitrogen ligands is much less developed. Our results present rare examples of such insertion chemistry in Pd(II) complexes with a monoanionic, bidentate nitrogen ligand.<sup>17,31</sup>

## Conclusions

Formazanate palladium complexes are accessible via either protonolysis or salt metathesis reactions, which in many cases was shown to lead to homoleptic bis(formazanate)palladium compounds (**2**) due to their thermodynamic stability. For complex **2**, a redox-series spanning 4 different oxidation states based on ligand-centered redox reactions is observed by cyclic voltammetry, highlighting the rich electrochemistry of formazanate ligands. Our attempts to synthesize mono(formazanate) analogues via salt metathesis point to the formation of a neutral, three-coordinate palladium methyl complex starting from the precursor [Pd(COD)(CH<sub>3</sub>)Cl], but this is only stable when a fourth ligand is available to complement the square planar coordination sphere around Pd. A first example of such a compound, the methylpalladate complex **5** (stabilized by Cl<sup>-</sup> coordination) was synthesized and structurally characterized. Preliminary studies show that Cl<sup>-</sup> dissociation allows investigation of the reaction chemistry of the (1)Pd(CH<sub>3</sub>)-fragment in **5**, as exemplified by CO, isocyanide and methyl acrylate insertion into the Pd-CH<sub>3</sub> bond. The lack of catalytic oligomerization/polymerization reactivity with these compounds is likely related to their sluggish olefin insertion kinetics, and poor thermal stability. Although the decomposition pathways are not known in detail, it appears that the unencumbered formazanate ligand used here does not provide sufficient steric protection around the metal center, and low-coordinate reaction intermediates can readily engage in bimolecular reactions leading to homoleptic complexes such as **2**, and/or other catalytically inactive species.

## Experimental Section

**General Considerations.** All manipulations were carried out under nitrogen or argon using standard glovebox, Schlenk, and vacuum-line techniques. For the synthesis of complex **2** and **3**, the solvents acetone, *n*-hexane and THF (Aldrich, anhydrous, 99.8 %) were used without further purification, while anhydrous dichloromethane was freshly distilled over CaH<sub>2</sub> under an argon atmosphere. For the synthesis of complex **5**, THF (Aldrich, anhydrous, 99.8%) was dried by percolation over columns of Al<sub>2</sub>O<sub>3</sub> (Fluka); hexane (Aldrich, anhydrous, 99.8%) was passed over columns of Al<sub>2</sub>O<sub>3</sub> (Fluka), BASF R3-11-supported Cu oxygen scavenger, and molecular sieves (Aldrich, 4 Å). NMR solvents were either used as received (CD<sub>2</sub>Cl<sub>2</sub>, Sigma-Aldrich), or vacuum transferred from Na/K alloy and stored under nitrogen (THF-*d*<sub>8</sub>, Euriso-top). Compounds **1H**<sup>32</sup> and **1K**<sup>20</sup> were synthesized according to literature procedures. [Pd(CH<sub>3</sub>)Cl(COD)] was either prepared according to the literature procedure,<sup>33</sup> or obtained commercially (99%, Strem Chemicals). Benzonitrile (Aldrich), HCl (37%, Fluka) and 1,5-*cis,cis*-cyclooctadiene (Fluka) (used for the synthesis of [Pd(CH<sub>3</sub>)Cl(COD)]), and tetrabutylammonium chloride (99%, Sigma-Aldrich), 4-methoxyphenyl isocyanide (97%, Sigma-Aldrich) and [Pd(CH<sub>3</sub>COO)<sub>2</sub>] (Engelhard Italy) were used as received. 1D and 2D NMR spectra were recorded on Varian Gemini 400, Mercury 400 or Inova 500 spectrometers. The resonances are reported in ppm (δ) and referenced to the residual solvent peak versus Si(CH<sub>3</sub>)<sub>4</sub>: CD<sub>2</sub>Cl<sub>2</sub> at δ 5.32 (<sup>1</sup>H) and δ 53.84 ppm (<sup>13</sup>C), THF-*d*<sub>8</sub> at δ 3.58 (<sup>1</sup>H) and δ 67.21 ppm (<sup>13</sup>C). The assignment of NMR resonances was aided by gradient-selected COSY, NOESY, HSQC, and/or HMBC experiments using standard pulse sequences.

The infrared spectrum of compound **2** was recorded on a Perkin–Elmer FT-IR 2000 spectrometer in transmission mode and the sample was prepared as a KBr pellet. The infrared

spectrum of compound **5** was recorded on a INTERSPEC FT-IR spectrometer in transmission mode under N<sub>2</sub> atmosphere and the sample was prepared by evaporation of a THF solution of the compound on KBr plates. Elemental analyses were performed at the Microanalytical Department of the University of Groningen. Cyclic voltammetry was performed using a three-electrode setup with a silver wire pseudoreference electrode and a platinum disk working electrode (CHI102, CH Instruments; diameter = 2 mm). The platinum working electrode was polished before the experiment using an alumina slurry (0.05 μm), rinsed with distilled water, and subjected to brief ultrasonication to remove any adhered alumina microparticles. The electrodes were then dried in an oven at 75 °C overnight to remove any residual traces of water. The CV data were calibrated by adding ferrocene or decamethylferrocene as a THF solution at the end of the experiments. There is no indication that the addition of ferrocene and or decamethylferrocene influences the electrochemical behavior of the products. All electrochemical measurements were performed at ambient temperatures under an inert N<sub>2</sub> atmosphere in THF containing 0.1 M [nBu<sub>4</sub>N][PF<sub>6</sub>] as the supporting electrolyte. Data were recorded with *Autolab NOVA* software (version 1.8 and version 2.0).

**Synthesis of [Pd(1)<sub>2</sub>] (2).** [Pd(CH<sub>3</sub>CO<sub>2</sub>)<sub>2</sub>] (1 eq, 100.0 mg, 0.45 mmol) was dissolved at room temperature in acetone (12 mL). After stirring for 30 min, the mixture was filtered on paper obtaining a brownish-red clear solution. The ligand **1H** (2 eq, 283.0 mg, 0.9 mmol) was added as a solid to the solution, which immediately became intensely red colored. The reaction mixture was stirred for 5 h at room temperature, observing a change of color towards darker tonality. After concentration of the mixture and storage at +4 °C overnight, a dark solid precipitated and it was filtered off and washed with cold acetone, affording 140.6 mg of product (0.19 mmol, 43 %). Single crystals suitable for X-ray diffraction were obtained by slow diffusion of *n*-hexane

into a chloroform solution of **2** at 4 °C. <sup>1</sup>H NMR (500 MHz, CD<sub>2</sub>Cl<sub>2</sub>, 25 °C): δ 8.04 (d, 4H, *p*-tolyl *o*-CH), 7.63 (d, 8H, Ph *o*-CH), 7.35 (d, 4H, *p*-tolyl *m*-CH), 7.10 (t, 8H, Ph *m*-CH), 7.01 (m, 4H, Ph *p*-CH), 2.47 (s, 3H, *p*-tolyl CH<sub>3</sub>) ppm. <sup>13</sup>C NMR\* (126 MHz, CD<sub>2</sub>Cl<sub>2</sub>, 25 °C) δ 129.04 (*p*-tolyl *m*-C), 128.06 (Ph *m*-C), 126.56 (Ph *p*-C), 124.61 (*p*-tolyl *o*-C), 123.21 (Ph *o*-C), 20.87 (*p*-tolyl CH<sub>3</sub>). Anal. calcd for C<sub>40</sub>H<sub>34</sub>N<sub>8</sub>Pd: C 65.53, H 4.67, N 15.28; found: C 65.46, H 4.70, N 15.14. IR: ν<sub>max</sub> = 1269 (stretch C-N), 1198 (stretch N-N) cm<sup>-1</sup>. MS (ESI, CH<sub>3</sub>Cl): *m/z* = 755.2 [M + Na<sup>+</sup>], 732.2 [M + H<sup>+</sup>]. \* <sup>13</sup>C NMR resonances taken from a HSQC experiment; quaternary carbons not listed.

**Reaction of [Pd(COD)(CH<sub>3</sub>)Cl] with **1K**: formation of [(**1**)Pd(μ-OH)]<sub>2</sub> (**3**).** [Pd(COD)(CH<sub>3</sub>)Cl] (50.0 mg, 1 eq, 0.19 mmol) was dissolved in a Schlenk flask, under inert atmosphere, in THF (7 mL) leading to a pale yellow solution. **1K** (94.5 mg, 0.5 eq, 0.095 mmol) was added to the solution leading to a violet reaction mixture that was stirred at room temperature for 30 min, observing that its color turned blue. After concentration and precipitation with *n*-hexane at +4 °C, a blue solid was obtained. The <sup>1</sup>H NMR spectrum showed the presence of two major species, **2** and **3** (in ratio 4:1 respectively).

Repeating the same reaction at 0 °C led to a mixture in which **3** was present as the major species based on <sup>1</sup>H NMR spectroscopy (**2**:**3** ratio = 0.25:1). From this crude material, we were able to obtain **3** in crystalline form by slow diffusion of *n*-hexane into an NMR solution in CD<sub>2</sub>Cl<sub>2</sub> at 4 °C. NMR data for **3**: <sup>1</sup>H NMR (500 MHz, CD<sub>2</sub>Cl<sub>2</sub>, 25 °C): δ 7.78 (d, 4H, *p*-tolyl *o*-CH), 7.68 (d, 8H, Ph *o*-CH), 7.24-7.14 (m, 16 H Ph *m*-CH; Ph *p*-CH; *p*-tolyl *m*-CH), 2.36 (s, 6H, *p*-tolyl CH<sub>3</sub>), -3.46 (s, 2H, μ-OH). <sup>13</sup>C NMR (126 MHz, CD<sub>2</sub>Cl<sub>2</sub>, 25 °C) δ = 129.16, (*p*-tolyl *m*-C), 128.94 (Ph *m*-C), 127.85 (Ph *p*-C), 124.66 (*p*-tolyl *o*-C), 123.94 (Ph *o*-C), 20.98 (*p*-tolyl CH<sub>3</sub>).

**Synthesis of [Bu<sub>4</sub>N][(1)Pd(CH<sub>3</sub>)Cl] (5).** Tetrabutylammonium chloride (54.2 mg, 1 eq, 0.195 mmol) was added to a pale yellow solution of [Pd(COD)(CH<sub>3</sub>)Cl] (50.0 mg, 1 eq, 0.195 mmol) in THF (15 mL). **1K** (96.0 mg, 0.5 eq, 0.0975 mmol) was slowly added as a solid to the reaction mixture while stirring. Immediately the reaction mixture turned blue-turquoise. After stirring for 2h the reaction mixture was filtered and slow diffusion of hexane into the THF solution at room temperature afforded 114.9 mg of [Bu<sub>4</sub>N][(1)Pd(CH<sub>3</sub>)Cl] (**5**) as blue crystals suitable for X-Ray diffraction (0.161 mmol 83%). <sup>1</sup>H NMR (500 MHz, THF-*d*<sub>8</sub>, 25 °C): δ 8.41 (d, 2H, Ph *o*-CH), 8.05 (d, 2H, Ph *o*-CH), 7.99 (d, 2H *p*-tolyl *o*-CH), 7.22-7.16 (m, 6H Ph and Ph' *m*-CH and *p*-tolyl *m*-CH), 7.00-6.95 (m, 2H Ph and Ph' *p*-CH), 3.19 (m, 8H, NBu<sub>4</sub><sup>+</sup> CH<sub>2</sub>), 2.36 (s, 3H, *p*-tolyl CH<sub>3</sub>), 1.49 (m, 8H, NBu<sub>4</sub><sup>+</sup> CH<sub>2</sub>), 1.28 (m, 8H, NBu<sub>4</sub><sup>+</sup> CH<sub>2</sub>) 0.88 (t, 12H, NBu<sub>4</sub><sup>+</sup> CH<sub>3</sub>) 0.02 (Pd-CH<sub>3</sub>). <sup>13</sup>C NMR (101 MHz, THF-*d*<sub>8</sub>, 25 °C) δ 156.0 (Ph' *ipso*-C), 155.1 (Ph *ipso*-C), 149.3 (NCN), 138.7 (*p*-tolyl *ipso*-C), 136.1 (*p*-tolyl *ipso*-CCH<sub>3</sub>), 129.6 (*p*-tolyl *m*-C), 128.4 (Ph and Ph' *m*-C), 125.8 (Ph and Ph' *p*-C), 125.6 (Ph *o*-C), 125.5 (Ph' *o*-C), 125.0 (*p*-tolyl *o*-C), 59.3 (NBu<sub>4</sub><sup>+</sup> CH<sub>2</sub>), 24.8 (NBu<sub>4</sub><sup>+</sup> CH<sub>2</sub>), 21.5 (*p*-tolyl *p*-C), 20.7 (NBu<sub>4</sub><sup>+</sup> CH<sub>2</sub>), 14.2 (NBu<sub>4</sub><sup>+</sup> CH<sub>3</sub>), -5.0 (Pd-CH<sub>3</sub>). Anal. calcd for C<sub>37</sub>H<sub>56</sub>N<sub>5</sub>ClPd: C 62.35, H 7.92, N 9.83; found: C 62.19, H 7.93, N 9.79. IR: ν<sub>max</sub> = 1276 cm<sup>-1</sup> (stretch C-N), 1188 cm<sup>-1</sup> (stretch N-N).

**Synthesis of [(1)Pd(CH<sub>3</sub>)(py)] (6).** Complex **5** (99.7 mg, 0.14 mmol) was dissolved in 3.5 mL of distilled DCM under argon atmosphere, to give a turquoise colored solution. A solution of pyridine (30 μL, 29.5 mg, 0.37 mmol) in DCM (2 mL) was added to the palladium complex under stirring, which gave an immediate color change to a deep blue solution. The reaction mixture was stirred for 3 hours, after which it was filtered over Celite. The filtrate was taken to dryness and redissolved in 2 mL of DCM, to which 14 mL hexane was added. Overnight, a solid precipitated which was filtered off and the filtrate was taken to dryness to afford **6** as a dark blue

solid (33.0 mg, 0.064 mmol, 46%).  $^1\text{H}$  NMR (500 MHz,  $\text{CD}_2\text{Cl}_2$ , 25 °C):  $\delta$  8.52 (d, 2H, pyridine CH(2,6)), 8.02 (d, 2H, Ph *o*-CH), 8.01 (d, 2H, *p*-Tol *o*-CH), 7.74 (d, 2H, Ph' *o*-CH), 7.60 (t, 1H, pyridine CH(4)), 7.39 (t, 2H, Ph *m*-CH), 7.26 (d, 2H, *p*-Tol *m*-CH), 7.19 (t, 1H, Ph *p*-CH), 7.13 (t, 2H, pyridine CH(3,5)), 7.09 (t, 2H, Ph *m*-CH), 6.93 (t, 1H, Ph *p*-CH), 2.42 (s, 3H, *p*-Tol *p*-CH<sub>3</sub>), 0.04 (s, 3H, Pd-CH<sub>3</sub>).  $^{13}\text{C}$  NMR\* (126 MHz,  $\text{CD}_2\text{Cl}_2$ , 25 °C):  $\delta$  152.86 (pyridine CH(2,6)), 137.46 (pyridine CH(4)), 129.21 (*p*-Tol *m*-CH), 128.41 (Ph' *m*-CH), 128.32 (Ph *m*-CH), 126.06 (Ph *p*-CH), 125.84 (Ph' *p*-CH), 125.25 (pyridine CH(3,5)), 124.93 (*p*-Tol *o*-CH & Ph *o*-CH), 123.72 (Ph' *o*-CH), 21.20 (*p*-Tol *p*-CH<sub>3</sub>), -0.35 (Pd-CH<sub>3</sub>). \*  $^{13}\text{C}$  NMR resonances taken from a HSQC experiment; quaternary carbons not listed. Anal. calcd for  $\text{C}_{26}\text{H}_{25}\text{N}_5\text{Pd}$ : C 60.76, H 4.90, N 13.63; found: C 60.76, H 5.14, N 13.08.

**NMR reaction of 5 with CO in THF-*d*<sub>8</sub> to give compound 7.** In a glovebox, compound 5 (5.8 mg,  $8.1 \cdot 10^{-3}$  mmol) was dissolved in a J. Young's NMR tube in THF-*d*<sub>8</sub>. The solution was frozen in liquid N<sub>2</sub> and the N<sub>2</sub> atmosphere inside the J. Young's NMR tube was removed at the schlenk line. Subsequently, the NMR tube was allowed to warm to room temperature and then was filled with 1 bar of CO, observing the solution turning to a darker shade of blue. The *in situ* formed product (7) was characterized via NMR spectroscopy at -40 °C. The first spectrum was recorded after 20 min from the addition of CO and shows that the starting material has been completely converted.  $^1\text{H}$  NMR (500 MHz, THF-*d*<sub>8</sub>, -40 °C):  $\delta$  8.37 (d, 2H, Ph or Ph' *o*-CH), 8.04 (d, 2H, *p*-tolyl *o*-CH), 7.97 (d, 2H, Ph or Ph' *o*-CH), 7.27-7.22 (m, 6H, *p*-tolyl *m*-CH, Ph and Ph' *m*-CH), 7.06 (t, 1H, Ph or Ph' *p*-CH) 7.01 (t, 1H, Ph or Ph' *p*-CH), 3.22 (m, 8H, NBu<sub>4</sub><sup>+</sup> CH<sub>2</sub>), 2.38 (6H, *p*-tolyl CH<sub>3</sub> and Pd-COCH<sub>3</sub>), 1.37 (m, 8H, NBu<sub>4</sub><sup>+</sup> CH<sub>2</sub>), 1.25 (m, 8H, NBu<sub>4</sub><sup>+</sup> CH<sub>2</sub>) 0.86 (t, 12H, NBu<sub>4</sub><sup>+</sup> CH<sub>3</sub>) ppm.  $^{13}\text{C}$  NMR (126 MHz, THF-*d*<sub>8</sub>, -40 °C):  $\delta$  235.8 (Pd-COCH<sub>3</sub>), 158.1 (Ph or Ph' *ipso*-C), 154.6 (Ph or Ph' *ipso*-C), 146.1 (NCN), 138.4 (*p*-tolyl *ipso*-



C), 136.4 (*p*-tolyl *ipso*-CCH<sub>3</sub>), 124.8 (Ph or Ph' *o*-CH), 124.8 (*p*-tolyl *o*-CH), 124.7 (d, 2H Ph or Ph' *o*-CH), 130.1 (*p*-tolyl *m*-CH) 128.7 (Ph or Ph' *m*-CH), 128.5 (Ph or Ph' *m*-CH), 126.5 (Ph or Ph' *p*-CH) 126.2 (Ph or Ph' *p*-CH), 58.4 (NBu<sub>4</sub><sup>+</sup> CH<sub>2</sub>), 37.4 (Pd-COCH<sub>3</sub>) 24.4 (NBu<sub>4</sub><sup>+</sup> CH<sub>2</sub>), 21.6 (*p*-tolyl CH<sub>3</sub>) 20.6 (NBu<sub>4</sub><sup>+</sup> CH<sub>2</sub>), 14.5 (NBu<sub>4</sub><sup>+</sup> CH<sub>3</sub>) ppm.

**NMR reaction of 5 with 4-methoxyphenyl isocyanide in THF-*d*<sub>8</sub> to give compound 8.** In a glovebox, 4-methoxyphenyl isocyanide (1 eq, 2.0 mg, 1.5·10<sup>-2</sup> mmol) was added as a solid to a J. Young's NMR tube containing a blue-turquoise THF-*d*<sub>8</sub> solution of **5** (1 eq, 10.7 mg, 1.5·10<sup>-2</sup> mmol). After recording a <sup>1</sup>H NMR spectrum at t = 30 min at -40 °C a second equivalent of isocyanide was added (2.0 mg, 1.5·10<sup>-2</sup> mmol) to the reaction mixture which turned to a darker shade of blue. The *in situ* formed product (**8**) was characterized via NMR spectroscopy at -40 °C. <sup>1</sup>H NMR (500 MHz, THF-*d*<sub>8</sub>, -40 °C): δ 8.18 (d, 2H Ph' *o*-CH), 7.76 (d, 2H Ph *o*-CH), 7.71 (d, 2H *p*-tolyl *o*-CH), 7.47 (t, 2H Ph' *m*-CH), 7.35 (t, 2H Ph *m*-CH), 7.24-7.15 (m, 6H, CNPhOCH<sub>3</sub> *o*-CH, Ph and Ph' *p*-CH, *p*-tolyl *m*-CH), 7.00 (d, 2H, CNPhOCH<sub>3</sub> *m*-CH), 6.83 (d, 2H, CH<sub>3</sub>CNPhOCH<sub>3</sub> *o*-CH), 6.55 (d, 2H, CH<sub>3</sub>CNPhOCH<sub>3</sub> *m*-CH), 3.81 (s, 3H, CNPhOCH<sub>3</sub>), 3.20 (s, 3H, CH<sub>3</sub>CNPhOCH<sub>3</sub>), 2.48 (s, 3H, CH<sub>3</sub>CNPhOCH<sub>3</sub>), 2.39 (s, 3H, *p*-tolyl CH<sub>3</sub>). <sup>13</sup>C NMR (126 MHz, THF-*d*<sub>8</sub>, -40 °C): δ 184.5 (CH<sub>3</sub>CNPhOCH<sub>3</sub>), 162.1 (CNPhOCH<sub>3</sub> *ipso*-COCH<sub>3</sub>), 157.0 (CH<sub>3</sub>CNPhOCH<sub>3</sub> *ipso*-COCH<sub>3</sub>), 156.8 (Ph' *ipso*-C), 156.4 (Ph *ipso*-C), 146.8 (NCN), 146.6 (CH<sub>3</sub>CNPhOCH<sub>3</sub> *ipso*-CNC), 141.3 (CNPhOCH<sub>3</sub>), 136.9 (*p*-tolyl *ipso*-CCH<sub>3</sub>), 136.6 (*p*-tolyl *ipso*-C), 129.8 (Ph' *m*-CH), 129.6 (*p*-tolyl *m*-CH), 129.0 (CNPhOCH<sub>3</sub> *o*-CH), 128.8 (Ph *m*-CH), 127.4 (Ph *p*-CH), 127.3 (Ph' *p*-CH), 125.5 (*p*-tolyl *o*-CH), 125.4 (Ph *o*-CH), 124.6 (Ph' *o*-CH), 121.7 (CH<sub>3</sub>CNPhOCH<sub>3</sub> *o*-CH), 119.5 (CNPhOCH<sub>3</sub> *ipso*-CNC), 115.9 (CNPhOCH<sub>3</sub> *m*-CH), 113.7 (CH<sub>3</sub>CNPhOCH<sub>3</sub> *m*-CH), 56.4 (CNPhOCH<sub>3</sub>), 54.7 (CH<sub>3</sub>CNPhOCH<sub>3</sub>), 35.9 (CH<sub>3</sub>CNPhOCH<sub>3</sub>), 21.6 (*p*-tolyl CH<sub>3</sub>).

**NMR reaction of 6 with CO in CD<sub>2</sub>Cl<sub>2</sub> to give compound 9.** Compound 6 (3.86 mg, 7.51 μmol) was placed in a NMR tube and dissolved in 0.75 mL CD<sub>2</sub>Cl<sub>2</sub> resulting in a turquoise solution. CO was bubbled through the solution for 10 minutes which resulted in a slight darkening of the solution to a dark blue color. The reaction was followed over the course of several hours, during which the reaction proceeded and after 200 minutes the reaction had almost reached completion (95% conversion). The *in situ* formed product (**9**) was characterized via NMR spectroscopy. <sup>1</sup>H NMR (400 MHz, CD<sub>2</sub>Cl<sub>2</sub>, 25 °C): δ 8.71 (d, 2H, pyridine CH(2,6)), 8.08 (d, 2H, *p*-tolyl *o*-CH), 8.03 (d, 2H, Ph *o*-CH), 7.59 (t, 1H, pyridine CH(4)), 7.57 (d, 2H, Ph' *o*-CH), 7.38 (t, 2H, Ph *m*-CH), 7.30 (d, 2H, *p*-tolyl *m*-CH), 7.19 (t, 1H, Ph *p*-CH), 7.14 (t, 2H, pyridine CH(3,5)), 7.05 (t, 2H, Ph' *m*-CH), 6.91 (t, 1H, Ph' *p*-CH), 2.44 (s, 3H, *p*-Tol *p*-CH<sub>3</sub>), 1.81 (m, 3H, Pd-COCH<sub>3</sub>) ppm. <sup>13</sup>C NMR\* (100 MHz, CD<sub>2</sub>Cl<sub>2</sub>, 25 °C): δ 151.73 (pyridine CH(2,6)), 137.61 (pyridine CH(4)), 128.97 (*p*-tolyl *m*-CH), 128.28 (Ph *m*-CH), 128.08 (Ph' *m*-CH), 126.34 (Ph *p*-CH), 125.70 (Ph' *p*-CH), 124.73 (*p*-tolyl *o*-CH), 124.33 (Ph *o*-CH), 124.56 (pyridine CH(3,5)), 122.77 (Ph' *o*-CH), 36.72 (Pd-COCH<sub>3</sub>), 20.82 (*p*-Tol *p*-CH<sub>3</sub>) ppm. \* <sup>13</sup>C NMR resonances taken from a HSQC experiment; quaternary carbons not listed.

**NMR reaction of 6 with methyl acrylate in CD<sub>2</sub>Cl<sub>2</sub> to give compound 10.** Compound 6 (3.80 mg, 7.4 μmol) was placed in a NMR tube and dissolved in 0.75 mL CD<sub>2</sub>Cl<sub>2</sub>, to which 1.35 μL (1.29 mg, 15 μmol) methyl acrylate was added. The reaction was followed over the course of several hours, during which the reaction proceeded very slowly. After 102 hours, the reaction had reached 87% conversion, and the product was characterized by NMR spectroscopy. Attempts to isolate the product by recrystallization were unsuccessful. <sup>1</sup>H NMR (500 MHz, CD<sub>2</sub>Cl<sub>2</sub>, 25 °C): δ 8.51 (d, 2H, pyridine CH(2,6)), 8.19 (d, 2H, Ph *o*-CH), 7.99 (d, 2H, *p*-Tol *o*-CH), 7.66 (d, 2H, Ph' *o*-CH), 7.56 (t, 1H, pyridine CH(4)), 7.45 (t, 2H, Ph *m*-CH), 7.27 (d, 2H, *p*-

Tol *m*-CH), 7.24 (t, 1H, Ph *p*-CH), 7.13 (t, 2H, pyridine CH(3,5)), 7.11 (t, 2H, Ph *m*-CH), 6.93 (t, 1H, Ph *p*-CH), 3.36 (s, 3H, -OCH<sub>3</sub>), 2.42 (s, 3H, *p*-Tol *p*-CH<sub>3</sub>), 2.34 (dd, 1H, CH), 1.25 (m, 1H, CH<sub>2</sub><sup>a</sup>), 1.06 (m, 1H, CH<sub>2</sub><sup>b</sup>), 0.70 (t, 3H, CH<sub>3</sub>). <sup>13</sup>C NMR\* (126 MHz, CD<sub>2</sub>Cl<sub>2</sub>, 25 °C): δ 152.30 (pyridine CH(2,6)), 137.34 (pyridine CH(4)), 128.90 (*p*-Tol *m*-CH), 128.21 (Ph *m*-CH), 128.10 (Ph' *m*-CH), 126.09 (Ph *p*-CH), 125.67 (Ph' *p*-CH), 125.03 (Ph *o*-CH), 124.36 (*p*-Tol *o*-CH), 124.34 (pyridine CH(3,5)), 123.19 (Ph' *o*-CH), 49.67 (-OCH<sub>3</sub>), 31.27 (C<sub>α</sub>H), 24.03 (C<sub>β</sub>H<sub>2</sub>), 20.79 (*p*-Tol *p*-CH<sub>3</sub>), 14.47 (C<sub>γ</sub>H<sub>3</sub>). \* <sup>13</sup>C NMR resonances taken from a HSQC experiment; quaternary carbons not listed.

**X-ray crystallography.** Single crystal data of **2** and **3** were collected at the X-ray diffraction beamline XRD1 of the ELETTRA Synchrotron, Trieste (Italy), using the rotating crystal method with a monochromatic wavelength of 0.7000 Å, on a Dectris Pilatus 2M detector. Measurements were performed at 100(2) K using a nitrogen stream cryo-cooler. Cell refinement, indexing and scaling of the data sets were performed using the CCP4 package,<sup>34</sup> and programs Denzo and Scalepack.<sup>35</sup> The structures were solved by direct methods and Fourier analyses and refined by the full-matrix least-squares method based on F<sup>2</sup> with all observed reflections.<sup>36</sup> All non-hydrogen atoms were refined with anisotropic displacement coefficients. For compound **5**, a single crystal was mounted on top of a cryoloop and transferred into the cold nitrogen stream (100 K) of a Bruker-AXS D8 Venture diffractometer. Data collection and reduction was done using the Bruker software suite APEX3.<sup>37</sup> The final unit cell was obtained from the xyz centroids of 9783 reflections after integration. A multiscan absorption correction was applied, based on the intensities of symmetry-related reflections measured at different angular settings (SADABS). The structures were solved by direct methods using SHELXT<sup>38</sup> and refinement of the structure was performed using SHELXL.<sup>39</sup> Refinement was frustrated by a disorder problem: the last two

C atoms of one of the butyl groups in the Bu<sub>4</sub>N cation showed unrealistically large anisotropic displacement parameters. A two-site occupancy model was applied, which refined to a s.o.f. of 0.66 for the major fraction. The hydrogen atoms were generated by geometrical considerations, constrained to idealised geometries and allowed to ride on their carrier atoms with an isotropic displacement parameter related to the equivalent displacement parameter of their carrier atoms. Crystal data and details on data collection and refinement are presented in Table 2.

**Table 2.** Crystallographic data for **2**, **3** and **5**.

	<b>2</b>	<b>3</b>	<b>5</b>
chem formula	C <sub>40</sub> H <sub>34</sub> N <sub>8</sub> Pd.CHCl <sub>3</sub>	C <sub>40</sub> H <sub>36</sub> N <sub>8</sub> O <sub>2</sub> Pd <sub>2</sub> .CH <sub>2</sub> Cl <sub>2</sub>	C <sub>37</sub> H <sub>56</sub> N <sub>5</sub> ClPd
M <sub>r</sub>	852.52	958.49	712.71
cryst syst	triclinic	triclinic	monoclinic
color, habit	dark brown, needle	blue, block	blue, block
space group	P -1	P -1	P 21/n
a (Å)	8.0390(16)	9.897(2)	14.8027(6)
b (Å)	8.1400(16)	12.993(3)	16.6849(6)
c (Å)	14.734(3)	16.703(3)	15.6639(6)
α (°)	98.99(3)	105.23(3)	90
β (°)	90.96(3)	106.50(3)	107.675(2)
γ (°)	99.37(3)	98.54(3)	90
V (Å <sup>3</sup> )	938.7(3)	1928.5(8)	3686.1(2)
Z	1	2	4
ρ <sub>calc</sub> , g.cm <sup>-3</sup>	1.508	1.651	1.284

Radiation [ $\text{\AA}$ ]	Mo $K_{\alpha}$ 0.700	Mo $K_{\alpha}$ 0.700	Mo $K_{\alpha}$ 0.71073
$\mu(\text{Mo } K_{\alpha})$ , $\text{mm}^{-1}$	0.750	1.119	0.607
F(000)	434	964	1504
Temp (K)	100(2)	100(2)	100(2)
$\theta$ range ( $^{\circ}$ )	1.38-30.00	1.65-29.54	2.89 – 27.17
data collected (h,k,l)	-11:11; -11:11; -21:21	-13:12; -18:18; -23:23	-18:19; -21:21; -20:19
no. of reflns collected	34320	58674	54583
no. of indepndt reflns	5604	11162	8160
Observed reflns	5600	10833	6732
$F_o \geq 2.0 \sigma (F_o)$			
R(F) (%)	2.77	3.68	5.70
wR(F <sup>2</sup> ) (%)	7.71	10.35	11.99
GooF	1.198	1.059	1.197
weighting a,b	0.0399, 0.6900	0.0526, 5.2674	0.0049, 16.4500
params refined	260	505	423
min, max resid dens	-1.296, 1.250	-2.442, 2.770	-0.922, 2.203

## ASSOCIATED CONTENT

**Supporting Information.** The following files are available free of charge. Crystallographic data for compounds **2**, **3** and **5** (CIF)

NMR and UV/Vis spectral data for all compounds, description of in-situ NMR reactions, cyclic voltammograms, details of DFT calculations (PDF)

## AUTHOR INFORMATION

### Corresponding Author

\* email address for E.O: edwin.otten@rug.nl

\* email address for B.M.: milaniba@units.it

### Author Contributions

The manuscript was written through contributions of all authors. All authors have given approval to the final version of the manuscript.

## ACKNOWLEDGMENT

The Netherlands Organisation for Scientific Research (NWO) is gratefully acknowledged for funding (VIDI grant to EO). This work was financially supported by Università degli Studi di Trieste (Finanziamento di Ateneo per progetti di ricerca scientifica; FRA 2015), by MIUR (PRIN 2015, no.20154X9ATP\_005). FM thanks COST Action CM1205 for supporting a short-term scientific mission. FdV is grateful for financial support from the Erasmus+ programme of the European Union. We would like to thank the Center for Information Technology of the University of Groningen for their support and for providing access to the Peregrine high performance computing cluster.

## REFERENCES

- (1) (a) Nakamura, A.; Ito, S.; Nozaki, K. Coordination–Insertion Copolymerization of Fundamental Polar Monomers *Chem. Rev.* **2009**, *109*, 5215. (b) Carrow, B. P.; Nozaki, K. Transition-Metal-Catalyzed Functional Polyolefin Synthesis: Effecting Control through Chelating Ancillary Ligand Design and Mechanistic Insights *Macromolecules* **2014**, *47*, 2541.
- (2) Johnson, L. K.; Killian, C. M.; Brookhart, M. New Pd(II)- and Ni(II)-Based Catalysts for Polymerization of Ethylene and  $\alpha$ -Olefins *J. Am. Chem. Soc.* **1995**, *117*, 6414.

(3) (a) Ittel, S. D.; Johnson, L. K.; Brookhart, M. Late-Metal Catalysts for Ethylene Homo- and Copolymerization *Chem. Rev.* **2000**, *100*, 1169. (b) Guan, Z.; Popeney, C. S. In *Metal Catalysts in Olefin Polymerization*; Guan, Z., Ed.; Springer Berlin Heidelberg: Berlin, Heidelberg, 2009, p 179. (c) Guo, L.; Dai, S.; Sui, X.; Chen, C. Palladium and Nickel Catalyzed Chain Walking Olefin Polymerization and Copolymerization *ACS Catalysis* **2016**, *6*, 428. (d) Guo, L.; Liu, W.; Chen, C. Late transition metal catalyzed [small alpha]-olefin polymerization and copolymerization with polar monomers *Mater. Chem. Front.* **2017**, *1*, 2487.

(4) (a) Durand, J.; Milani, B. The role of nitrogen-donor ligands in the palladium-catalyzed polyketones synthesis *Coord. Chem. Rev.* **2006**, *250*, 542. (b) Rix, F. C.; Rachita, M. J.; Wagner, M. I.; Brookhart, M.; Milani, B.; Barborak, J. C. Palladium(ii)-catalyzed copolymerization of styrenes with carbon monoxide: mechanism of chain propagation and chain transfer *Dalton Trans.* **2009**, 8977. (c) Meduri, A.; Montini, T.; Ragaini, F.; Fornasiero, P.; Zangrando, E.; Milani, B. Palladium-Catalyzed Ethylene/Methyl Acrylate Cooligomerization: Effect of a New Nonsymmetric  $\alpha$ -Diimine *ChemCatChem* **2013**, *5*, 1170. (d) Rosar, V.; Meduri, A.; Montini, T.; Fini, F.; Carfagna, C.; Fornasiero, P.; Balducci, G.; Zangrando, E.; Milani, B. Analogies and Differences in Palladium-Catalyzed CO/Styrene and Ethylene/Methyl Acrylate Copolymerization Reactions *ChemCatChem* **2014**, *6*, 2403. (e) Rosar, V.; Montini, T.; Balducci, G.; Zangrando, E.; Fornasiero, P.; Milani, B. Palladium-Catalyzed Ethylene/Methyl Acrylate Co-Oligomerization: The Effect of a New Nonsymmetrical  $\alpha$ -Diimine with the 1,4-Diazabutadiene Skeleton *ChemCatChem* **2017**, *9*, 3402.

(5) Nakamura, A.; Anselment, T. M. J.; Claverie, J.; Goodall, B.; Jordan, R. F.; Mecking, S.; Rieger, B.; Sen, A.; van Leeuwen, P. W. N. M.; Nozaki, K. Ortho-Phosphinobenzenesulfonate:

A Superb Ligand for Palladium-Catalyzed Coordination–Insertion Copolymerization of Polar Vinyl Monomers *Acc. Chem. Res.* **2013**, *46*, 1438.

(6) Younkin, T. R.; Connor, E. F.; Henderson, J. I.; Friedrich, S. K.; Grubbs, R. H.; Bansleben, D. A. Neutral, Single-Component Nickel (II) Polyolefin Catalysts That Tolerate Heteroatoms *Science* **2000**, *287*, 460.

(7) Zhu, D.; Budzelaar, P. H. M. N-Aryl [small beta]-diiminate complexes of the platinum metals *Dalton Trans.* **2013**, *42*, 11343.

(8) (a) Nineham, A. W. The Chemistry of Formazans and Tetrazolium Salts *Chem. Rev.* **1955**, *55*, 355. (b) Sigeikin, G. I.; Lipunova, G. N.; Pervova, I. G. Formazans and their metal complexes *Russ. Chem. Rev.* **2006**, *75*, 885.

(9) (a) Frolova, N.; Vatsadze, S.; Zavodnik, V.; Rakhimov, R.; Zyk, N. Pyridine-containing nickel(II) bis-formazanates: Synthesis, structure, and electrochemical study *Russ. Chem. Bull.* **2006**, *55*, 1810. (b) Gilroy, J. B.; Patrick, B. O.; McDonald, R.; Hicks, R. G. Transition Metal Complexes of 3-Cyano- and 3-Nitroformazans *Inorg. Chem.* **2008**, *47*, 1287.

(10) (a) Siedle, A. R.; Pignolet, L. H. Formazanylpalladium compounds. Synthesis and structure of bis(1,3,5-tri-p-tolylformazanyl)palladium *Inorg. Chem.* **1980**, *19*, 2052. (b) Gilroy, J. B.; Ferguson, M. J.; McDonald, R.; Hicks, R. G. Synthesis and characterization of palladium complexes of 3-nitroformazans *Inorg. Chim. Acta* **2008**, *361*, 3388. (c) Zaïdman, A. V.; Pervova, I. G.; Rezinskikh, Z. G.; Lipunov, I. N.; Slepukhin, P. A. Synthesis and X-ray diffraction study of palladium(II) 1,3-diphenyl-5-(benzothiazol-2-yl)formazanate *Cryst. Reports* **2010**, *55*, 424.



(11) (a) Chang, M.-C.; Dann, T.; Day, D. P.; Lutz, M.; Wildgoose, G. G.; Otten, E. The Formazanate Ligand as an Electron Reservoir: Bis(Formazanate) Zinc Complexes Isolated in Three Redox States *Angew. Chem. Int. Ed.* **2014**, *53*, 4118. (b) Chang, M. C.; Otten, E. Synthesis and ligand-based reduction chemistry of boron difluoride complexes with redox-active formazanate ligands *Chem. Commun.* **2014**, *50*, 7431. (c) Chang, M.-C.; Otten, E. Reduction of (Formazanate)boron Difluoride Provides Evidence for an N-Heterocyclic B(I) Carbenoid Intermediate *Inorg. Chem.* **2015**, *54*, 8656. (d) Travieso-Puente, R.; Broekman, J. O. P.; Chang, M.-C.; Demeshko, S.; Meyer, F.; Otten, E. Spin-Crossover in a Pseudo-tetrahedral Bis(formazanate) Iron Complex *J. Am. Chem. Soc.* **2016**, *138*, 5503. (e) Chang, M. C.; Chantzis, A.; Jacquemin, D.; Otten, E. Boron difluorides with formazanate ligands: redox-switchable fluorescent dyes with large stokes shifts *Dalton Trans.* **2016**, *45*, 9477. (f) Mondol, R.; Snoeken, D. A.; Chang, M.-C.; Otten, E. Stable, crystalline boron complexes with mono-, di- and trianionic formazanate ligands *Chem. Commun.* **2017**, *53*, 513.

(12) (a) Gilroy, J. B.; Ferguson, M. J.; McDonald, R.; Patrick, B. O.; Hicks, R. G. Formazans as  $\beta$ -diketiminato analogues. Structural characterization of boratetetrazines and their reduction to borataverdazyl radical anions *Chem. Commun.* **2007**, 126. (b) Barbon, S. M.; Price, J. T.; Reinkeluers, P. A.; Gilroy, J. B. Substituent-Dependent Optical and Electrochemical Properties of Triarylformazanate Boron Difluoride Complexes *Inorg. Chem.* **2014**, *53*, 10585. (c) Maar, R.; Barbon, S. M.; Sharma, N.; Groom, H.; Luyt, L. G.; Gilroy, J. B. Evaluation of Anisole-Substituted Boron Difluoride Formazanate Complexes for Fluorescence Cell Imaging *Chem. Eur. J.* **2015**, *21*, 15589. (d) Hesari, M.; Barbon, S. M.; Staroverov, V. N.; Ding, Z.; Gilroy, J. B. Efficient electrochemiluminescence of a readily accessible boron difluoride formazanate dye *Chem. Commun.* **2015**, *51*, 3766. (e) Barbon, S. M.; Staroverov, V. N.; Gilroy, J. B. Structurally

Diverse Boron–Nitrogen Heterocycles from an N<sub>2</sub>O<sub>2</sub>– Formazanate Ligand *Angew. Chem. Int. Ed.* **2017**, *56*, 8173.

(13) Kabir, E.; Wu, C.-H.; Wu, J. I. C.; Teets, T. S. Heteroleptic Complexes of Cyclometalated Platinum with Triarylformazanate Ligands *Inorg. Chem.* **2016**, *55*, 956.

(14) Chang, M.-C.; Roewen, P.; Travieso-Puente, R.; Lutz, M.; Otten, E. Formazanate Ligands as Structurally Versatile, Redox-Active Analogues of  $\beta$ -Diketiminates in Zinc Chemistry *Inorg. Chem.* **2015**, *54*, 379.

(15) (a) Kokatam, S.-L.; Chaudhuri, P.; Weyhermüller, T.; Wieghardt, K. Molecular and electronic structure of square planar complexes [PdII(tbpy)(LIPN,O)]<sup>0</sup>, [PdII(tbpy)(LISQN,O)](PF<sub>6</sub>), and [PdII(tbpy)(LIBQN,O)](PF<sub>6</sub>)(BF<sub>4</sub>)·2CH<sub>2</sub>Cl<sub>2</sub>: an o-aminophenolato based ligand centered, three-membered redox series *Dalton Trans.* **2007**, 373.

(b) Kokatam, S.; Weyhermüller, T.; Bothe, E.; Chaudhuri, P.; Wieghardt, K. Structural Characterization of Four Members of the Electron-Transfer Series [PdII(L)<sub>2</sub>]<sub>n</sub> (L = o-Iminophenolate Derivative; n = 2<sup>-</sup>, 1<sup>-</sup>, 0, 1<sup>+</sup>, 2<sup>+</sup>). Ligand Mixed Valency in the Monocation and Monoanion with S = 1/2 Ground States *Inorg. Chem.* **2005**, *44*, 3709.

(16) Milani, B.; Anzilutti, A.; Vicentini, L.; Sessanta o Santi, A.; Zangrando, E.; Geremia, S.; Mestroni, G. Bis-Chelated Palladium(II) Complexes with Nitrogen-Donor Chelating Ligands Are Efficient Catalyst Precursors for the CO/Styrene Copolymerization Reaction *Organometallics* **1997**, *16*, 5064.

(17) Lin, B.-L.; Bhattacharyya, K. X.; Labinger, J. A.; Bercaw, J. E. Competitive Benzene C–H Bond Activation versus Olefin Insertion in a (Monomethyl)palladium(II)  $\beta$ -Diketimate Complex *Organometallics* **2009**, *28*, 4400.

(18) Tian, X.; Goddard, R.; Pörschke, K.-R. ( $\beta$ -Diketiminato)palladium Complexes *Organometallics* **2006**, *25*, 5854.

(19) (a) Hadzovic, A.; Janetzko, J.; Song, D. Novel dinuclear and trinuclear palladium [small beta]-diiminate complexes containing amido-chloro double-bridges *Dalton Trans.* **2008**, 3279.

(b) Hadzovic, A.; Song, D. Syntheses, Structures, and Reactivities of Novel Palladium  $\beta$ -Diiminate–Acetate Complexes *Inorg. Chem.* **2008**, *47*, 12010. (c) Annibale, V. T.; Lund, L. M.; Song, D. Unusual transmetallation-induced formation of a C<sub>2</sub>-symmetric tetrapallada-macrocycle *Chem. Commun.* **2010**, *46*, 8261. (d) Annibale, V. T.; Tan, R.; Janetzko, J.; Lund, L. M.; Song, D. Palladium  $\beta$ -diiminate chemistry: Reactivity towards monodentate ligands and arylboronic acids *Inorg. Chim. Acta* **2012**, *380*, 308.

(20) Travieso-Puente, R.; Chang, M.-C.; Otten, E. Alkali metal salts of formazanate ligands: diverse coordination modes as a result of the nitrogen-rich [NNC<sub>2</sub>NN] ligand backbone *Dalton Trans.* **2014**, *43*, 18035.

(21) Carrying out the reaction in CD<sub>2</sub>Cl<sub>2</sub> also results in formation of [Pd(COD)(CH<sub>3</sub>)<sub>2</sub>]: identical NMR shifts as those reported by Jordan and co-workers are observed.

(22) (a) Rudler-Chauvin, M.; Rudler, H. Chimie organometallique: VII. Nouvelle methode de preparation de CODPdMe<sub>2</sub> *J. Organomet. Chem.* **1977**, *134*, 115. (b) Foley, S. R.; Stockland, R. A.; Shen, H.; Jordan, R. F. Reaction of Vinyl Chloride with Late Transition Metal Olefin Polymerization Catalysts *J. Am. Chem. Soc.* **2003**, *125*, 4350.

(23) (a) Kogut, E.; Zeller, A.; Warren, T. H.; Strassner, T. Structure and Dynamics of Neutral  $\beta$ -H Agostic Nickel Alkyls: A Combined Experimental and Theoretical Study *J. Am. Chem. Soc.*

**2004**, 126, 11984. (b) Wiencko, H. L.; Kogut, E.; Warren, T. H. Neutral  $\beta$ -diketiminato nickel(II) monoalkyl complexes *Inorg. Chim. Acta* **2003**, 345, 199.

(24) (a) Amatore, C.; Jutand, A. Anionic Pd(0) and Pd(II) Intermediates in Palladium-Catalyzed Heck and Cross-Coupling Reactions *Acc. Chem. Res.* **2000**, 33, 314. (b) Kolter, M.; Böck, K.; Karaghiosoff, K.; Koszinowski, K. Anionic Palladium(0) and Palladium(II) Ate Complexes *Angew. Chem. Int. Ed.* **2017**, 56, 13244.

(25) Hadzovic, A.; Song, D. Synthesis, Characterization, and Reactivity of a Versatile Dinuclear Palladium  $\beta$ -Diiminate Complex *Organometallics* **2008**, 27, 1290.

(26) Shen, H.; Jordan, R. F. Reaction of Vinyl Chloride with Cationic Palladium Acyl Complexes *Organometallics* **2003**, 22, 1878.

(27) Mecking, S.; Johnson, L. K.; Wang, L.; Brookhart, M. Mechanistic Studies of the Palladium-Catalyzed Copolymerization of Ethylene and  $\alpha$ -Olefins with Methyl Acrylate *J. Am. Chem. Soc.* **1998**, 120, 888.

(28) Guironnet, D.; Caporaso, L.; Neuwald, B.; Göttker-Schnetmann, I.; Cavallo, L.; Mecking, S. Mechanistic Insights on Acrylate Insertion Polymerization *J. Am. Chem. Soc.* **2010**, 132, 4418.

(29) Tian, G.; Boone, H. W.; Novak, B. M. Neutral Palladium Complexes as Catalysts for Olefin–Methyl Acrylate Copolymerization: A Cautionary Tale *Macromolecules* **2001**, 34, 7656.

(30) (a) Vlaar, T.; Ruijter, E.; Maes, B. U. W.; Orru, R. V. A. Palladium-Catalyzed Migratory Insertion of Isocyanides: An Emerging Platform in Cross-Coupling Chemistry *Angew. Chem. Int. Ed.* **2013**, 52, 7084. (b) Qiu, G.; Ding, Q.; Wu, J. Recent advances in isocyanide insertion

chemistry *Chem. Soc. Rev.* **2013**, *42*, 5257. (c) Boyarskiy, V. P.; Bokach, N. A.; Luzyanin, K. V.; Kukushkin, V. Y. Metal-Mediated and Metal-Catalyzed Reactions of Isocyanides *Chem. Rev.* **2015**, *115*, 2698.

(31) Olson, J. A.; Paulose, T. A. P.; Wennek, P.; Quail, J. W.; Foley, S. R. Synthesis, structure and norbornene polymerization activity of a bulky  $\beta$ -diketiminato palladium(II) complex *Inorg. Chem. Commun.* **2008**, *11*, 1297.

(32) Gilroy, J. B.; Ferguson, M. J.; McDonald, R.; Patrick, B. O.; Hicks, R. G. Formazans as beta-diketiminate analogues. Structural characterization of boratatetrazines and their reduction to borataverdazyl radical anions *Chem. Commun.* **2007**, 126.

(33) Rulke, R. E.; Ernsting, J. M.; Spek, A. L.; Elsevier, C. J.; van Leeuwen, P. W. N. M.; Vrieze, K. NMR study on the coordination behavior of dissymmetric terdentate trinitrogen ligands on methylpalladium(II) compounds *Inorg. Chem.* **1993**, *32*, 5769.

(34) Collaborative Computational Project Number 4 The CCP4 suite: programs for protein crystallography *Acta Cryst. D* **1994**, *50*, 760.

(35) Otwinowski, Z.; Minor, W. In *International Tables for Crystallography Volume F: Crystallography of biological macromolecules*; Rossmann, M. G., Arnold, E., Eds.; Springer Netherlands: Dordrecht, 2001, p 226.

(36) Sheldrick, G. A short history of SHELX *Acta Cryst. A* **2008**, *64*, 112.

(37) Bruker. *APEX3, SAINT and SADABS*. Bruker AXS Inc., Madison, Wisconsin, USA. **2016**.

(38) Sheldrick, G. SHELXT - Integrated space-group and crystal-structure determination *Acta Cryst. A* **2015**, *71*, 3.

(39) Sheldrick, G. Crystal structure refinement with SHELXL *Acta Cryst. C* **2015**, *71*, 3.

TOC graphic

